Electronic Supplementary Information for

Chloromethyl-Modified Ru(II) Complexes Enabling Large pH Jumps at Low Concentrations through Photoinduced Hydrolysis

Na Tian,[ab] Weize Sun, [ab] Yang Feng, [ab] Xusheng Guo, [ab] Jian Lu, [ab] Chao Li,[a] Yuanjun Hou,[a] Xuesong Wang,*[ab] Qianxiong Zhou,*[a]
[a]Key Laboratory of Photochemical Conversion and Optoelectronic Material, Technical Institute of Physics and Chemistry, Chinese Academy of Sciences, Beijing 100190, P. R. China.
[b] University of Chinese Academy of Sciences, Beijing 100049, P. R. China.
E-mail: xswang@mail.ipc.ac.cn
E-mail: zhouqianxiong@mail.ipc.ac.cn

Experimental section

Materials

$RuCl_3 \cdot 3H_2O$, 2,2'-bipyridine (bpy), 4,4'-bis(chloromethyl)-2,2'-bipyridine(bcm-bpy), 1,10-phenanthroline monohydrate (phen), 4,4'-bis(hydroxymethyl)-2,2'-bipyridine (bhm-bpy),4-methylumbelliferyl phosphate (MUP)，7-hydroxy-4-methylcoumarin (MU), and acid phosphatase (from wheat germ) were purchased from Sigma Aldrich.

Instruments

^1H NMR spectra were determined on a Bruker DMX-400 MHz spectrophotometer. High-resolution ESI mass spectrometry (HR ESI-MS) spectra were recorded on a Brucker APEX IV (7.0T) FT_MS. UV-vis absorption spectra were obtained on a Shimadzu UV-1601 spectrophotometer. Emission spectra were performed on a Hitachi F-4600 fluorescence spectrophotometer. pH measurements were determined on PHSJ-3F pH meter from Shanghai INESA Scientific Instrument Co., Ltd. Light intensity was measured by a light meter (Newport 842-PE). In experiments associated with irradiation, an LED lamp (520 ± 10 nm) was used as light source.

Synthesis

The synthesis and detailed characterization were reported in our previous work.[1]

Theoretical calculations

All calculations were performed using the Gaussian 09 (G09) program package[2] employing the DFT method with Becke's three-parameter hybrid functional and Lee–Yang–Parr's gradient corrected correlation functional (B3LYP).[3] The LanL2DZ basis set and effective core potential were used for Ru atom, and the 6-31 G** basis set was applied for H, C, N and Cl. The geometries of the complexes were optimized in H_2O using the conductive polarizable continuum model (CPCM).

Photoacid quantum yield measurement

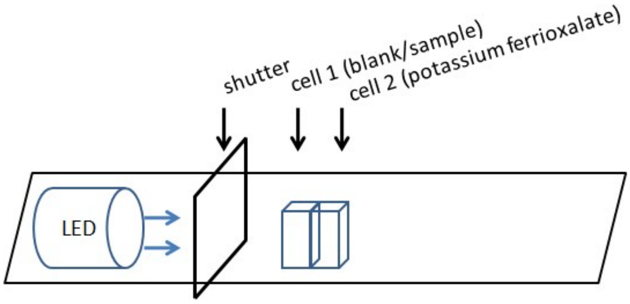

The simplified experimental apparatus is shown above. A 470 nm LED which emits collimated light and is power adjustable is used as the light source. Potassium ferrioxalate (0.15 M in H_2O) is used as the chemical actinometer.[4] Under light irradiation, potassium ferrioxalate will decompose, forming Fe^{2+}. The quantity of Fe^{2+} can be monitored by conversion to colored tris-phenanthroline complex (ε = 11100 L $mol^{-1}cm^{-1}$ at λ_{max} = 510 nm). The quantum yield (Φ_r) at 470 nm is 0.93. The mean fraction of 470 nm light absorbed by Potassium ferrioxalate (0.15 M) is measured to be about 60% (F). A pH meter (PHSJ-3F) is used to measure the H^+ concentrations. The pH values before irradiation are all about 6.6.

First, a blank cell (1 cm optical length, cell 1) with 2.1 ml (V_1) H_2O was put in front of another same cell (cell 2) loading 2.1 ml (V_1) potassium ferrioxalate (0.15 M). After irradiation for 5 s, 0.35 ml (V_2) of buffered phenanthroline (0.1%) was added in cell 2. The absorbance at 510 nm was measured as A1.

Then, similar operations were carried out using a sample cell containing complexes **1-3** (50 μM) instead of the blank one. After irradiation for 5 s, the pH value (P) of cell 1 was measured by a pH meter. 0.35 ml of buffered phenanthroline (0.1%) was added in cell 2. The absorbance at 510 nm was measured as A_2.

The mole of H^+ formed in the irradiated sample is given by

$$\text{mole } H^+ = (10^{-P}-10^{-6.6})\times V_1\times 10^{-3},$$

and the mole of 470 nm photons absorbed by the irradiated sample is given by

$$mole\ Photon_{abs} = \frac{\left(\frac{A_2 - A_1}{\varepsilon}\right) \times (V_1 + V_2) \times 10^{-3}}{\Phi_r \times F},$$

Thus the photoacid quantum yield can be calculated by $$\Phi_{PAG} = \frac{mole\ H^+}{mole\ Photon_{abs}}$$

The measurements were carried out for three times for each complex, and the raw data were listed as below.

	P	A_1	A_2	Φ_{PAG}	
1-1	4.89	0.280	0.387	0.63	0.62 ± 0.01
1-2	5.00	0.292	0.376	0.62	
1-3	5.10	0.294	0.360	0.62	
2-1	5.06	0.287	0.354	0.67	0.65 ± 0.02
2-2	5.04	0.290	0.364	0.63	
2-3	4.91	0.289	0.389	0.64	
3-1	4.95	0.269	0.364	0.61	0.61 ± 0.01
3-2	4.92	0.278	0.379	0.62	
3-3	4.89	0.282	0.392	0.61	

Enzyme activity studies

A solution containing acid phosphatase (0.08 mg/mL), MUP (83.3 μM), complex **3** (10 μM) and NaCl (150 mM) was adjusted to pH 8.0 by addition of NaOH. Upon irradiation with 520 nm LED for 90 s, the absorption spectra were recorded every 30 seconds.

The concentrations of MU were estimated according to the reported method.[5] Briefly, solutions containing complex **3** (10 μM) were irradiated with 520 nm LED for 90 s, then MUP and MU were added in the range from 0 μM to 20 μM for MU and 83.3 μM to 63.3 μM for MUP. The absorption at 370 nm was recorded and compared with that of the hydrolysis results above.

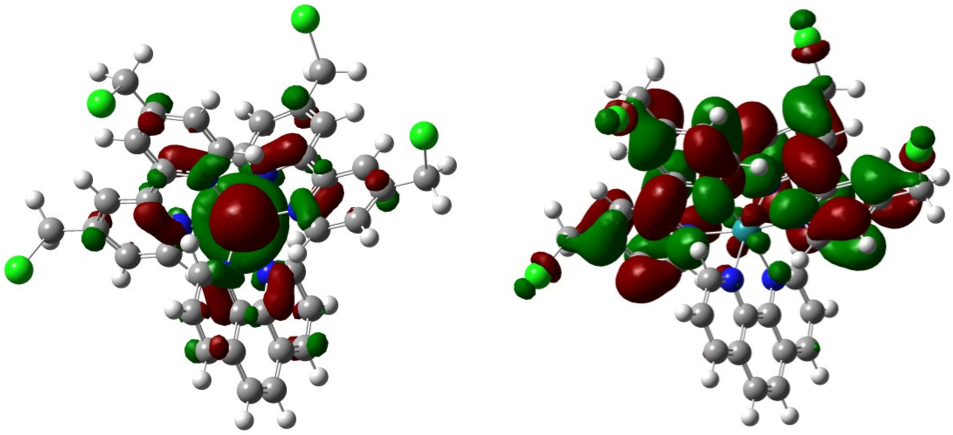

Figure S1. HOMO (left) and LUMO (right) of **2**.

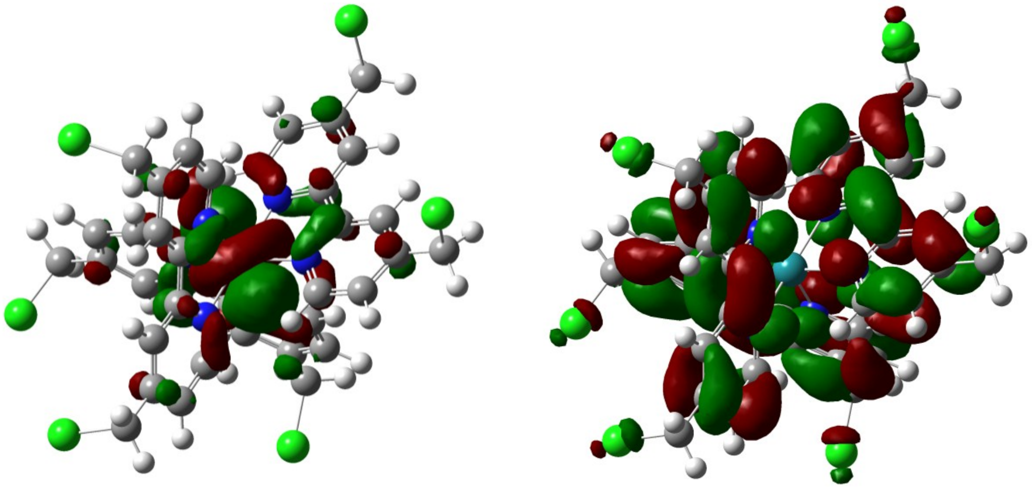

Figure S2. HOMO (left) and LUMO (right) of **3**.

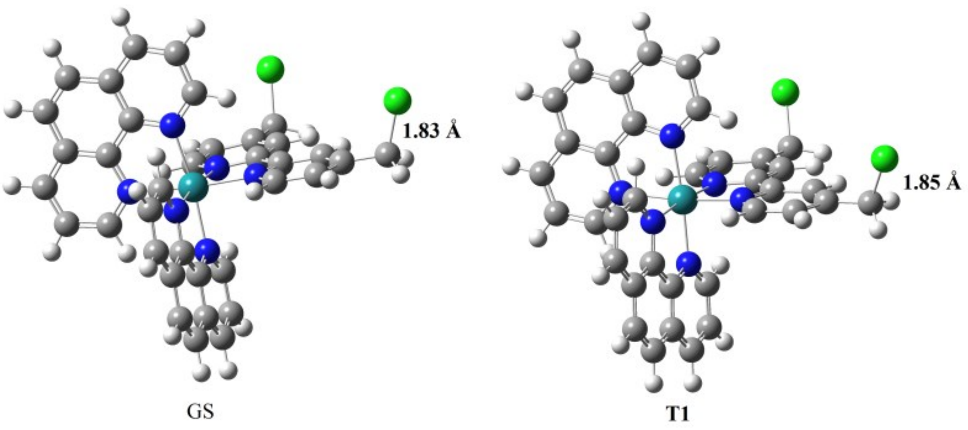

Figure S3. C-Cl bond lengths of **1**in the ground state(GS) and the lowest triplet state (T1).

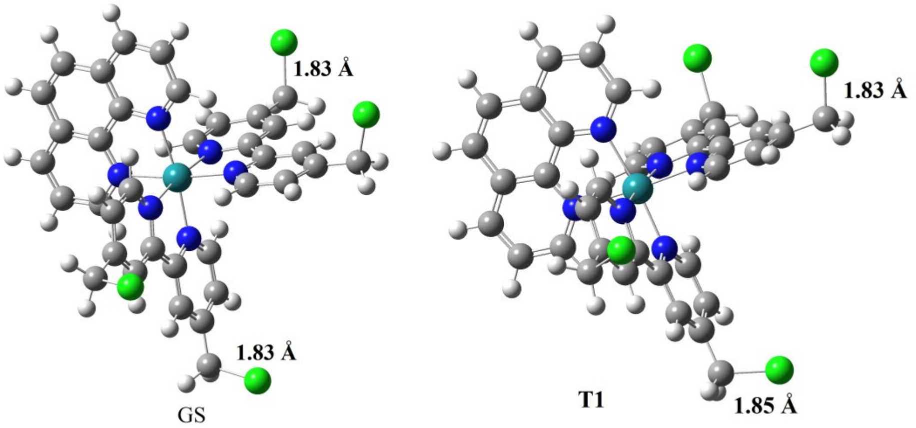

Figure S4. C-Cl bond lengths of **2** in the ground state (GS) and the lowest triplet state (T1).

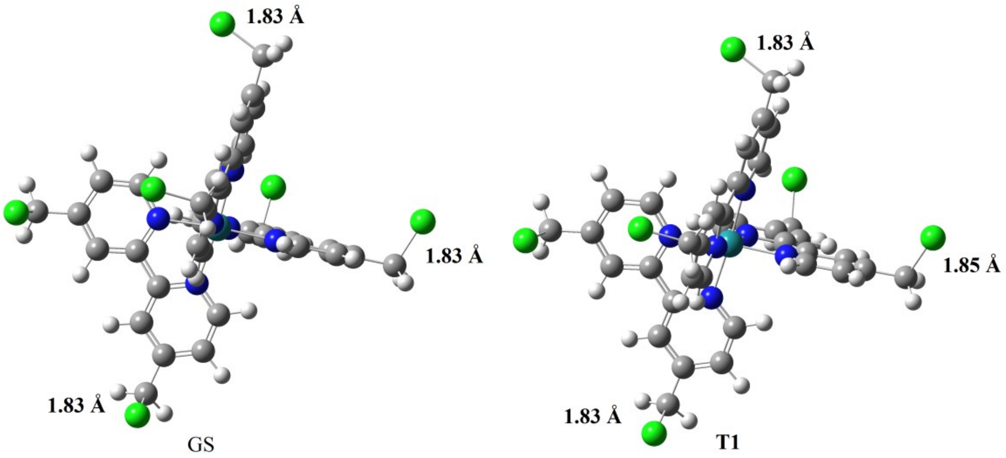

Figure S5. C-Cl bond lengths of **3** in the ground state (GS) and the lowest triplet state (T1).

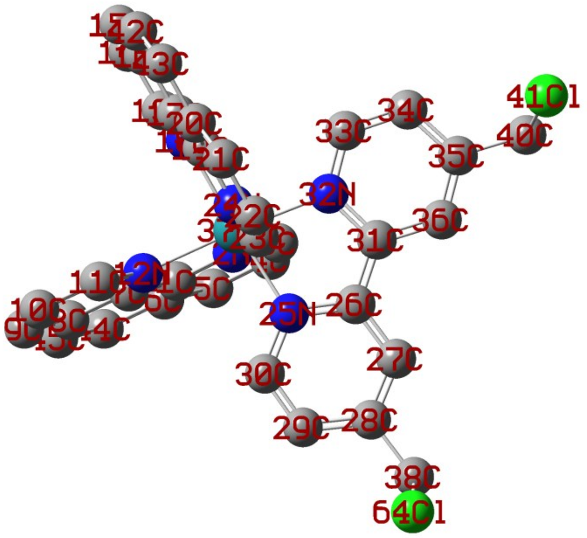

Figure S6. Atom numbering of **1**.

Table S1. Selected Mulliken charges (hydrogens summed to heavy atoms) of atoms on bcm-bpy ligand for complex **1** in GS and T1 states. (detailed atom numbering of **1,** see Figure S6).

Atom numbering	GS	T1
25N	-0.53	-0.62
26C	0.29	0.27
27C	0.05	0.01
28C	0.13	0.12
29C	0.04	-0.01
30C	0.27	0.26
31C	0.29	0.27
32N	-0.53	-0.62
33C	0.27	0.25
34C	0.04	-0.01
35C	0.13	0.12
36C	0.05	0.01
38C	0.05	0.03
40C	0.05	0.03
41Cl	-0.10	-0.14
64Cl	-0.10	-0.14

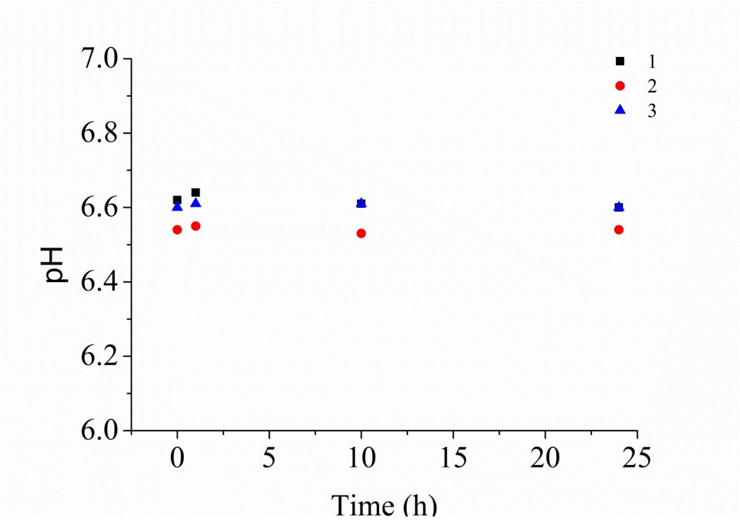

Figure S7. pH value changes of **1-3** (10 μM) solutions in H_2O for 24 h in the dark.

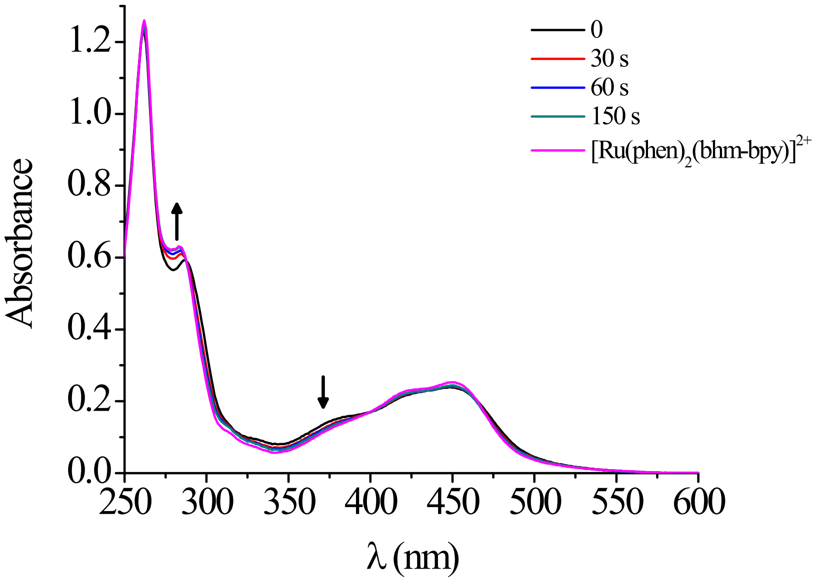

Figure S8. Absorption spectra changes of **1** (20 μM) in H_2O upon irradiation (λ_{irr} = 520 nm), compared with that of [Ru(phen)$_2$(bhm-bpy)]$^{2+}$ (20 μM in H_2O).

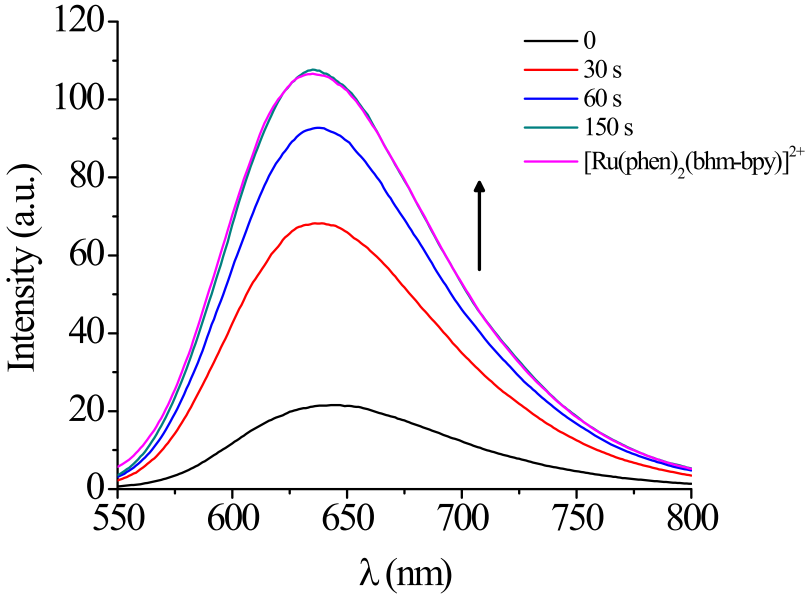

Figure S9. Emission spectra (λ_{ex} = 450 nm) changes of **1** (20 μM) in H_2O upon irradiation (λ_{irr} = 520 nm), compared with that of [Ru(phen)$_2$(bhm-bpy)]$^{2+}$ (20 μM in H_2O).

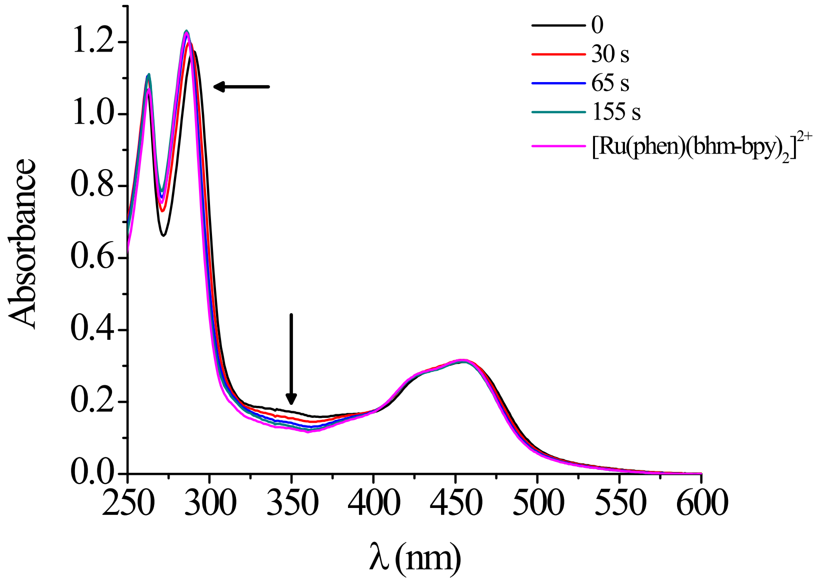

Figure S10. Absorption spectra changes of **2** (20 μM) in H_2O upon irradiation (λ_{irr} = 520 nm), compared with that of [Ru(phen)(bhm-bpy)$_2$]$^{2+}$ (20 μM in H_2O).

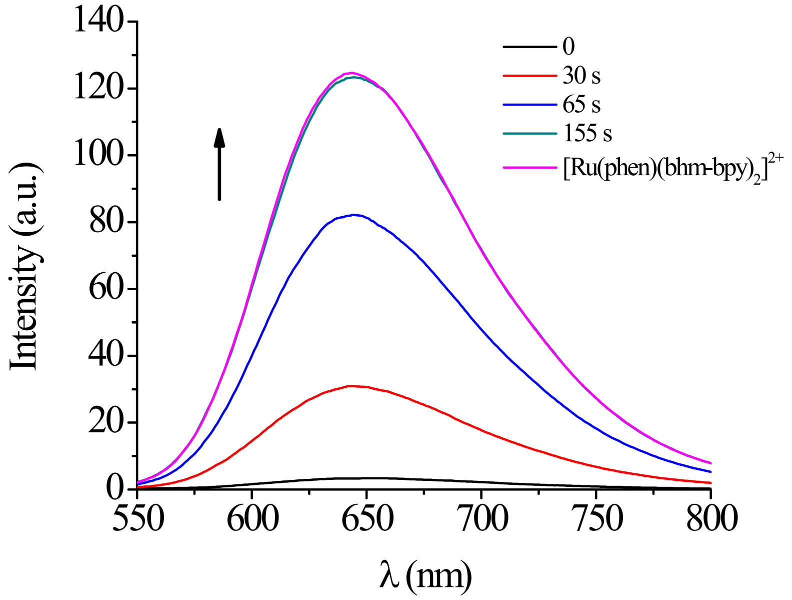

Figure S11. Emission spectra (λ_{ex} = 450 nm) changes of **2** (20 μM) in H_2O upon irradiation (λ_{irr} = 520 nm), compared with that [Ru(phen)(bhm-bpy)$_2$]$^{2+}$ (20 μM in H_2O).

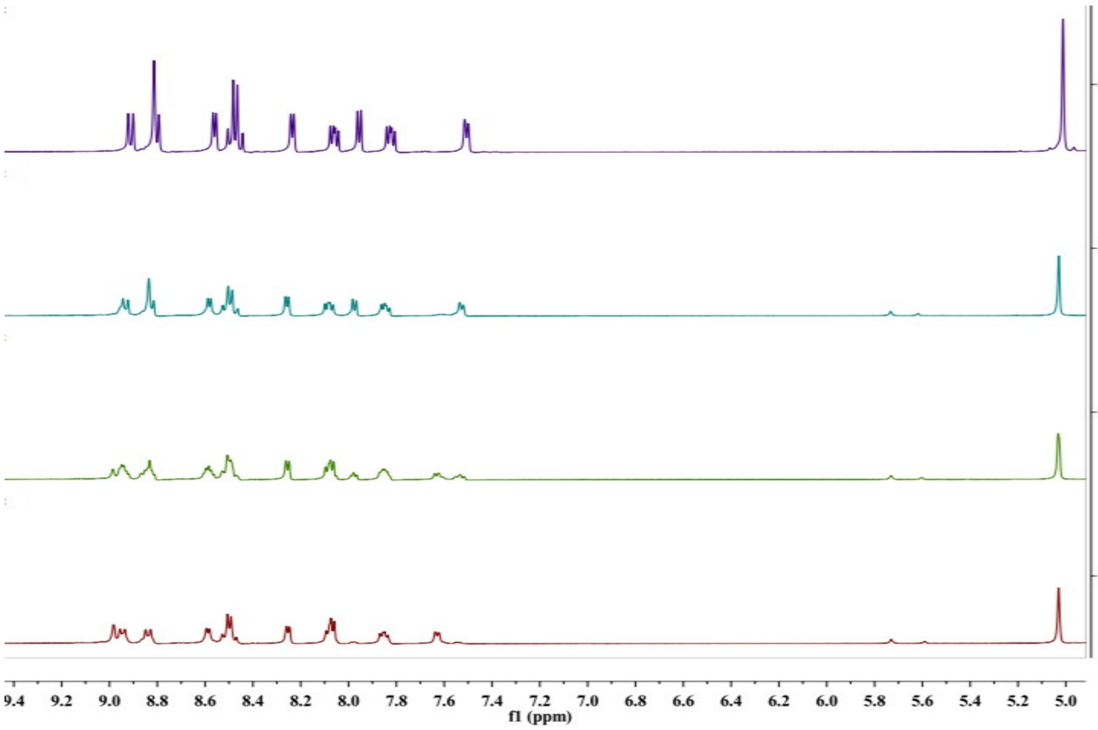

Figure S12. ^{1}H NMR spectra changes of **1** in D_2O: (1) before irradiation, (2-3) irradiation (λ_{irr} = 520 nm) for 5 min and 20 min, (4) ^{1}H NMR spectrum of $[Ru(phen)_2(bhm\text{-}bpy)]^{2+}$.

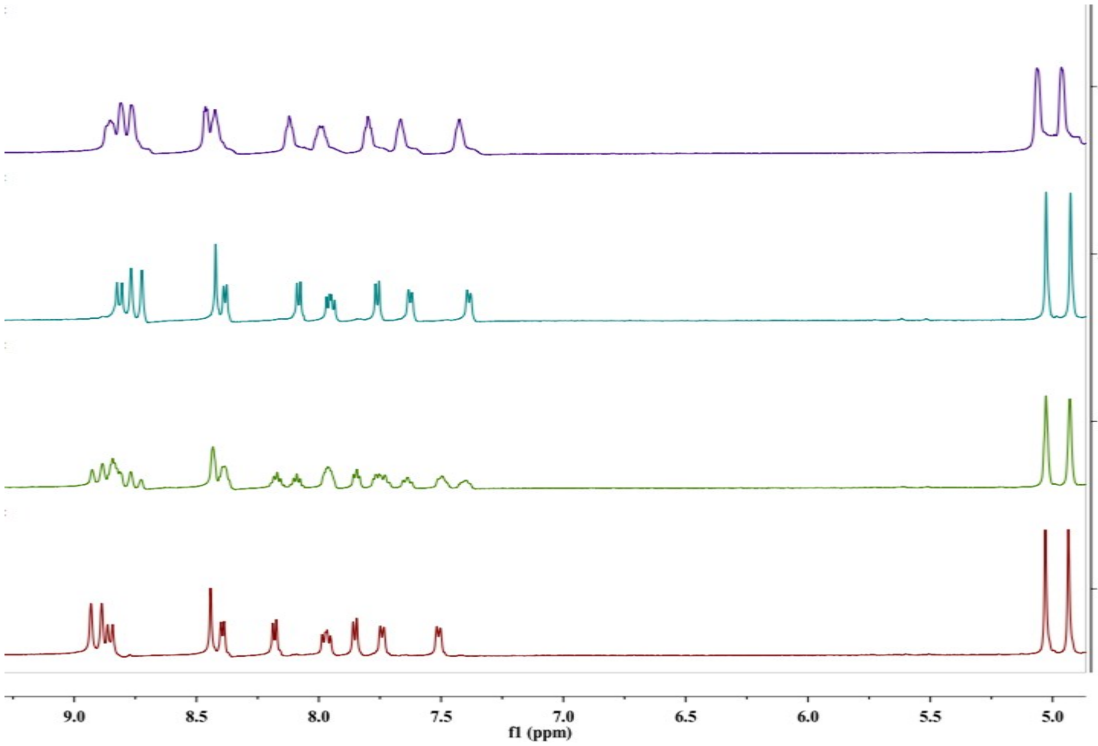

Figure S13. ^{1}H NMR spectra changes of **2** in D_2O: (1) before irradiation, (2-3) irradiation (λ_{irr} = 520 nm) for 5 min and 20 min, (4) ^{1}H NMR spectrum of $[Ru(phen)(bhm\text{-}bpy)_2]^{2+}$.

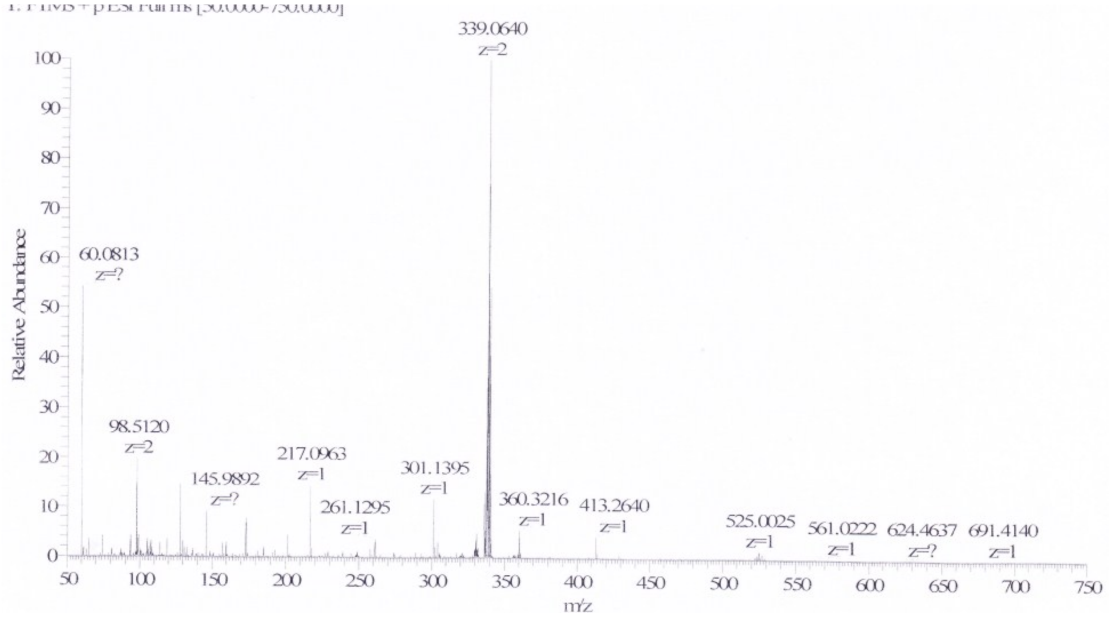

Figure S14. HR ESI-MS spectrum of **1** after irradiation for 10 min (λ_{irr} = 520 nm) in H_2O. The m/z peak of 339.0640 can be ascribed to the product with two hydroxymethyl groups (cal. m/z = 339.0658).

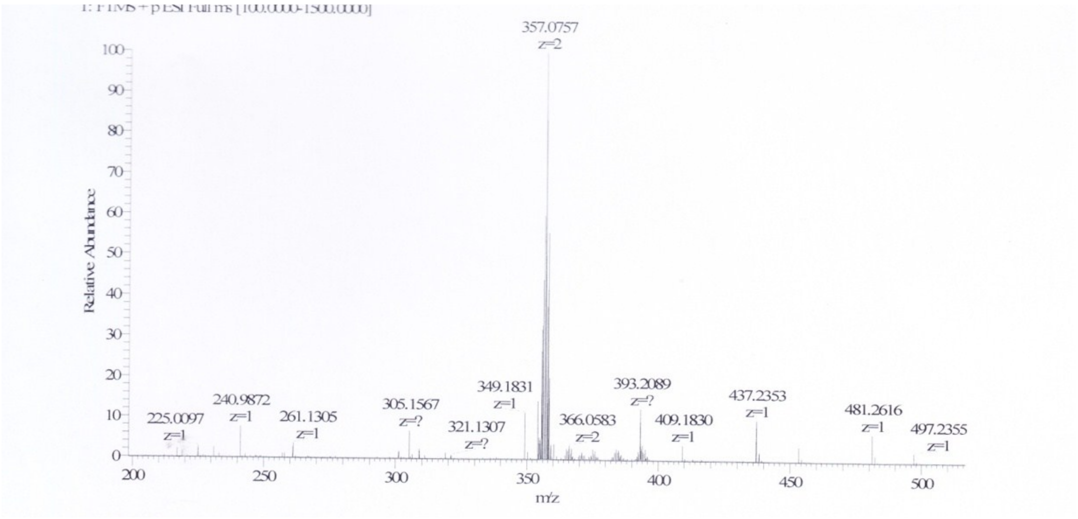

Figure S15. HR ESI-MS spectrum of **2** after irradiation for 10 min (λ_{irr} = 520 nm) in H_2O. The m/z peak of 357.0757 can be ascribed to the product with four hydroxymethyl groups (cal. m/z = 357.0764).

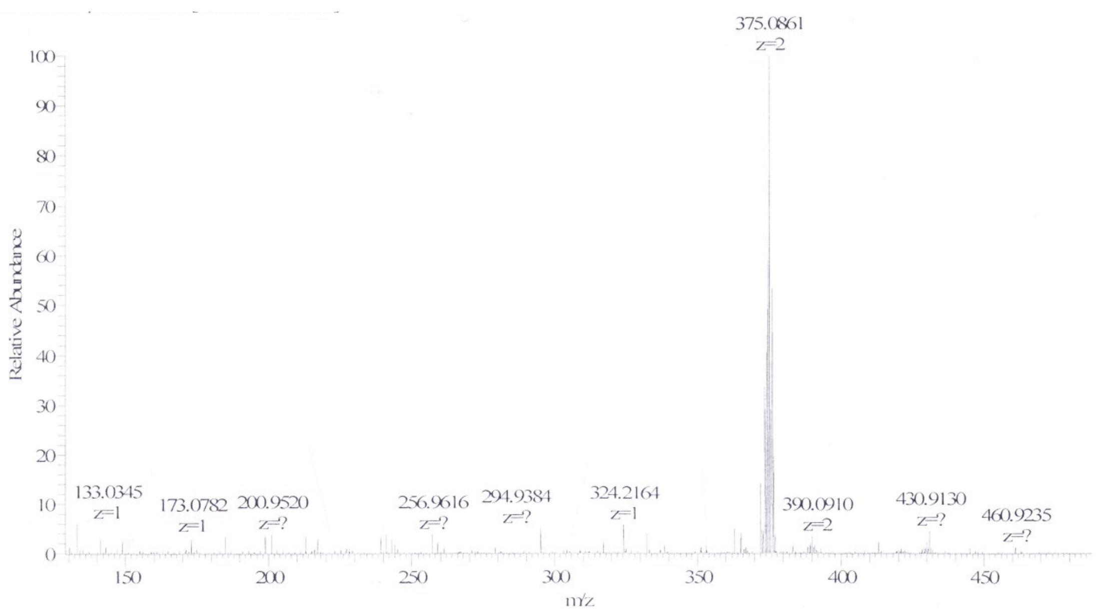

Figure S16. HR ESI-MS spectrum of **3** after irradiation for 10 min (λ_{irr} = 520 nm) in H_2O. The m/z peak of 375.0861 can be ascribed to the product with six hydroxymethyl groups (cal. m/z = 375.0869).

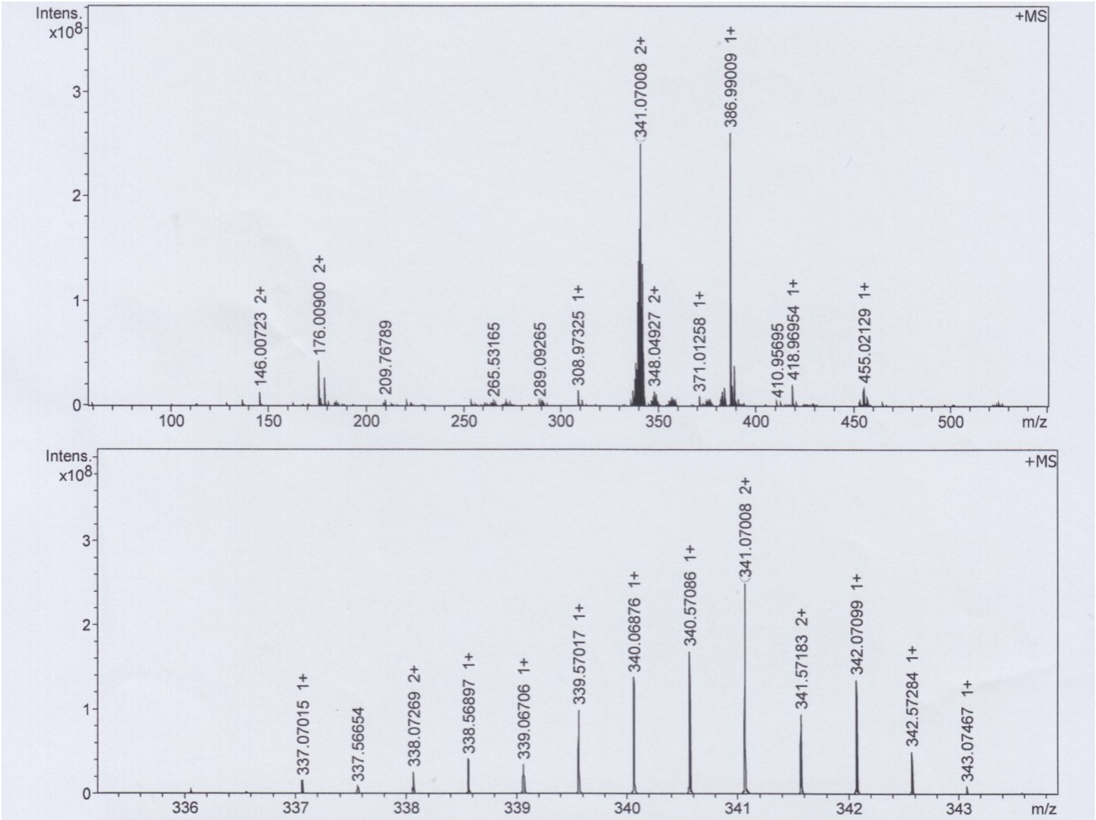

Figure S17. HR ESI-MS spectrum of **1** after irradiation for 10 min (λ_{irr} = 520 nm) in $H_2{}^{18}O$. The m/z peak of 341.07008 can be ascribed to the product with two ^{18}OH groups (cal. m/z = 341.07011).

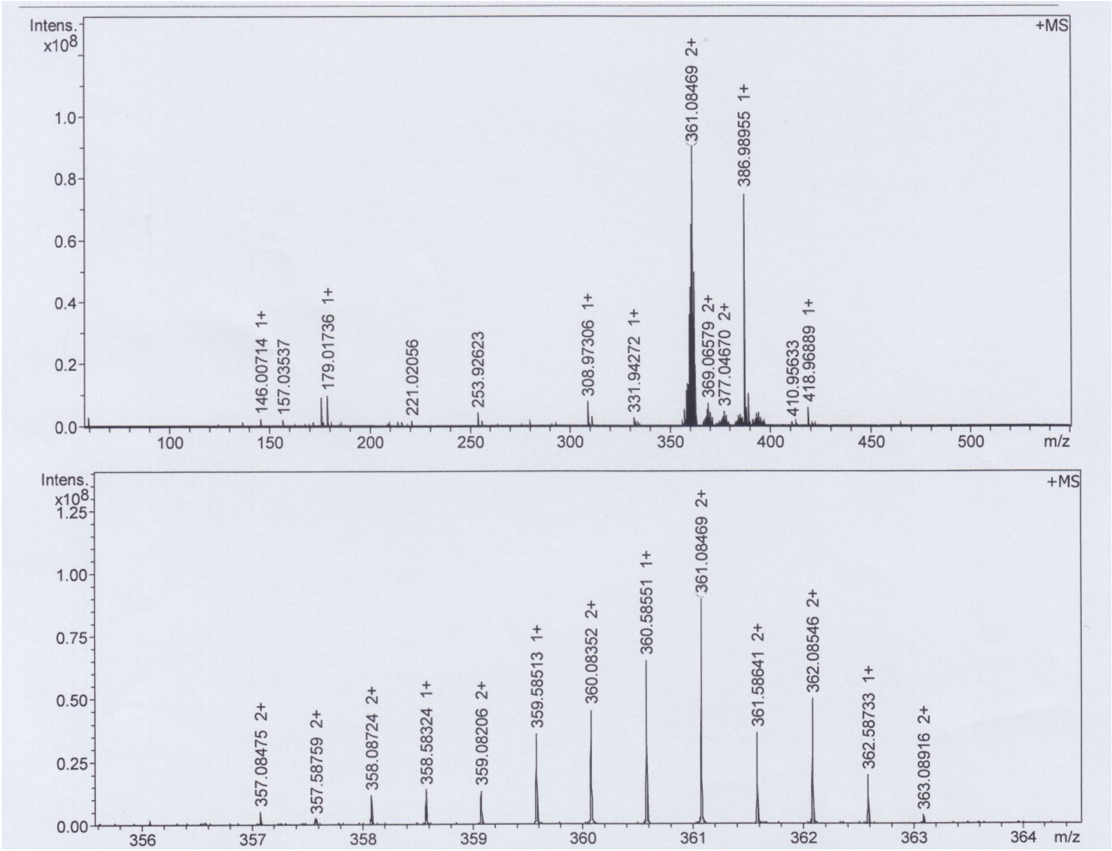

Figure S18. HR ESI-MS spectrum of **2** after irradiation for 10 min (λ_{irr} = 520 nm) in $H_2{}^{18}O$. The m/z peak of 361.08469 can be ascribed to the product with four ^{18}OH groups (cal. m/z = 361.08492).

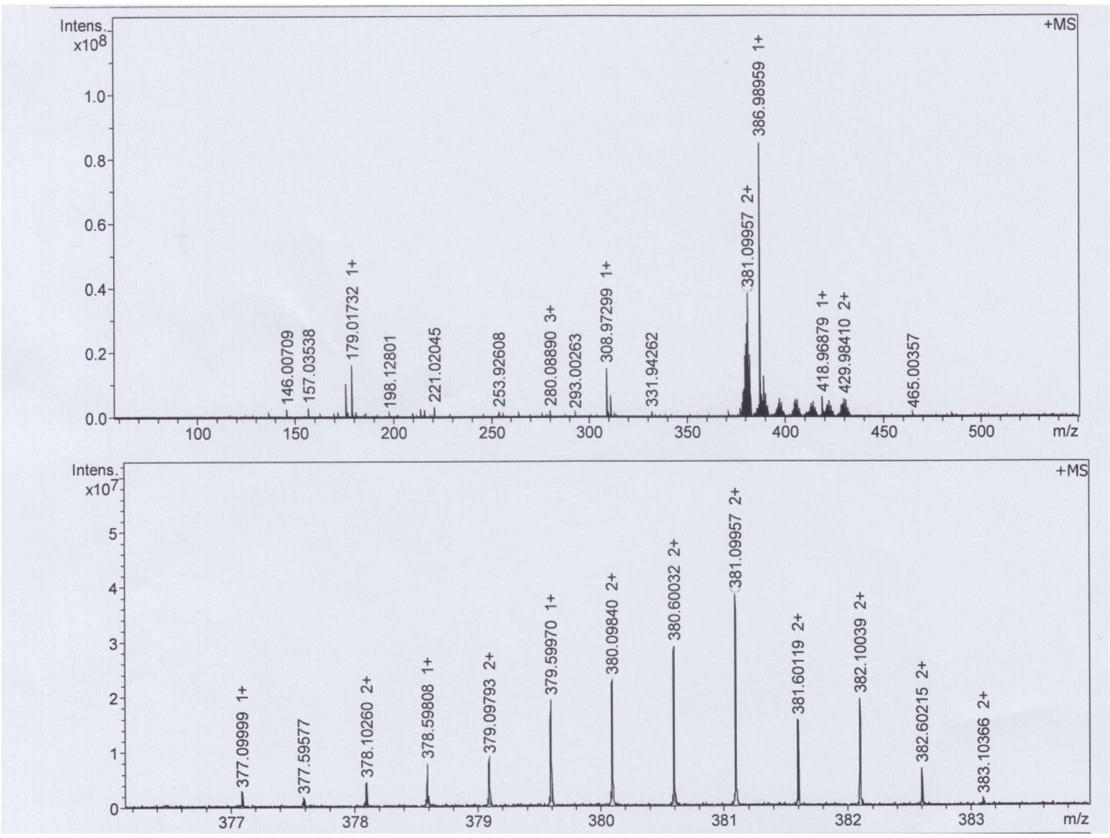

Figure S19. HR ESI-MS spectrum of **3** after irradiation for 10 min (λ_{irr} = 520 nm) in $H_2{}^{18}O$. The m/z peak of 381.09957 can be ascribed to the product with six ^{18}OH groups (cal. m/z = 381.09975).

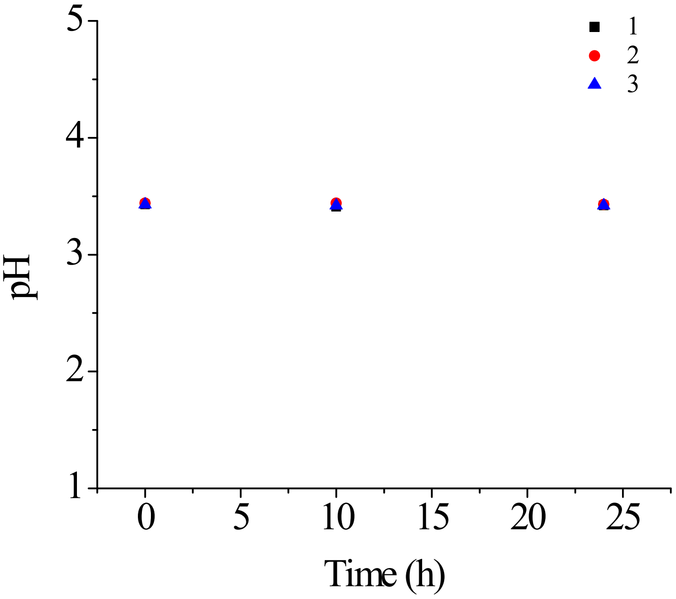

Figure S20. pH values of **1-3** (10 μM) in GSH (1 mM) aqueous solutions for 24 h in the dark.

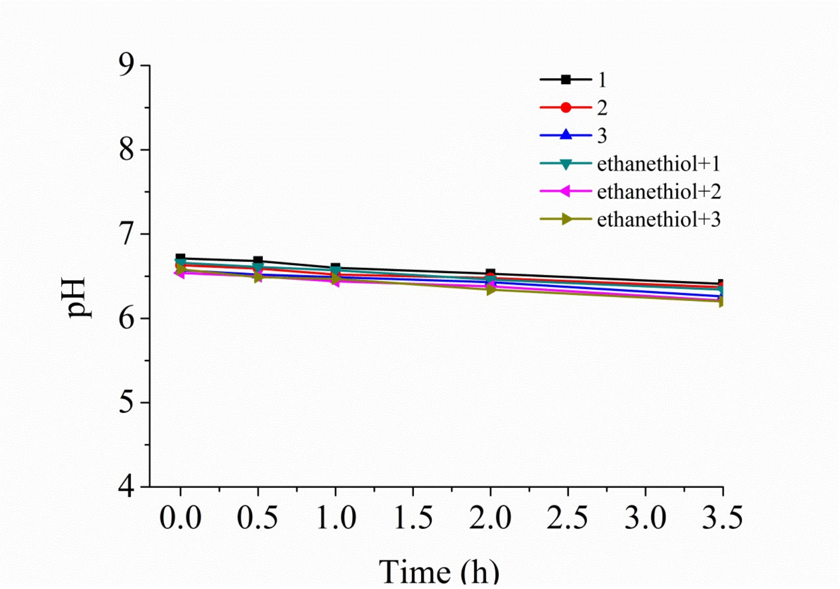

Figure S21. pH values of **1-3** solutions (10 μM in H_2O) in the absence or presence of ethanethiol (1 mM) in the dark and under 37 ^{o}C.

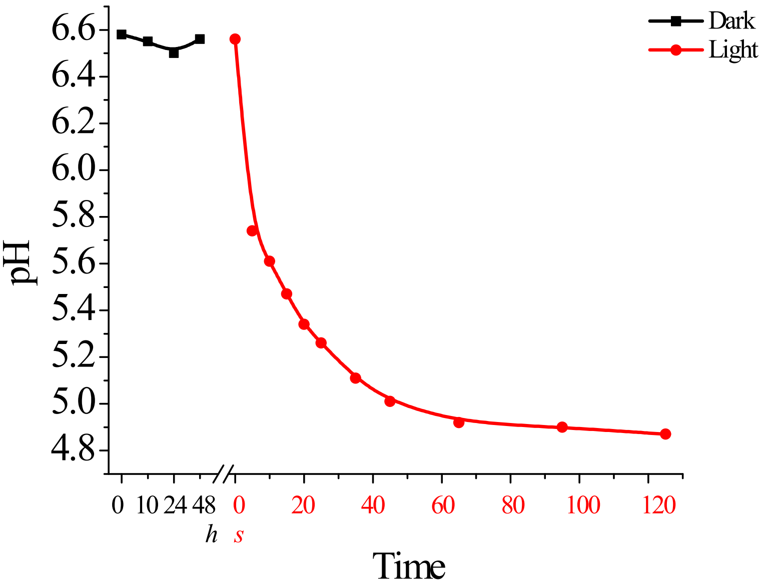

Figure S22. pH values of **1** solution (10 μM in H_2O) in the presence of ethanethiol (1 mM) in the dark (0-48 h, dark line) and under irradiation (λ_{irr} = 520 nm, 0-130 seconds, red line).

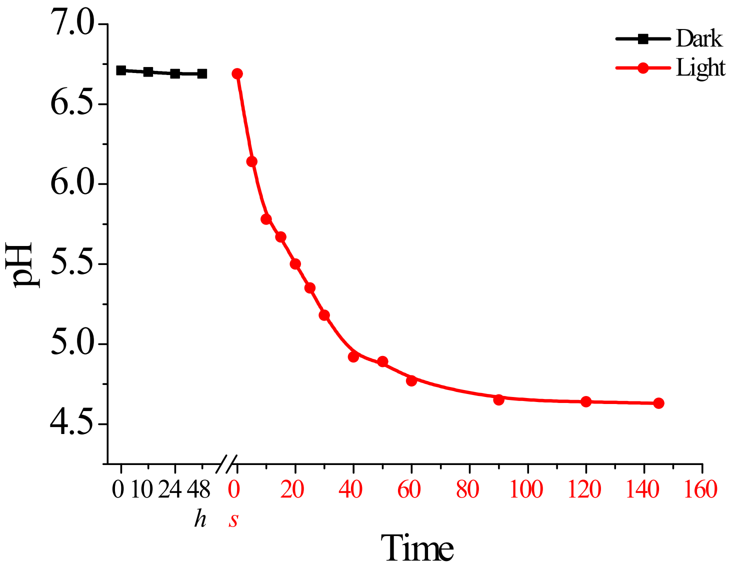

Figure S23. pH values of **2** solution (10 μM in H_2O) in the presence of ethanethiol (1 mM) in the dark (0-48 h, dark line) and under irradiation (λ_{irr} = 520 nm, 0-150 seconds, red line).

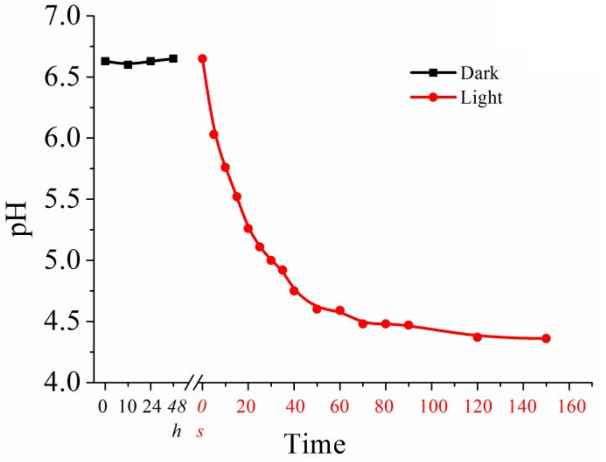

Figure S24. pH values of **3** (10 μM in H_2O) in the presence of ethanethiol (1 mM) in the dark (0-48 h, dark line) or under irradiation (λ_{irr}= 520 nm, 0-150 seconds, red line).

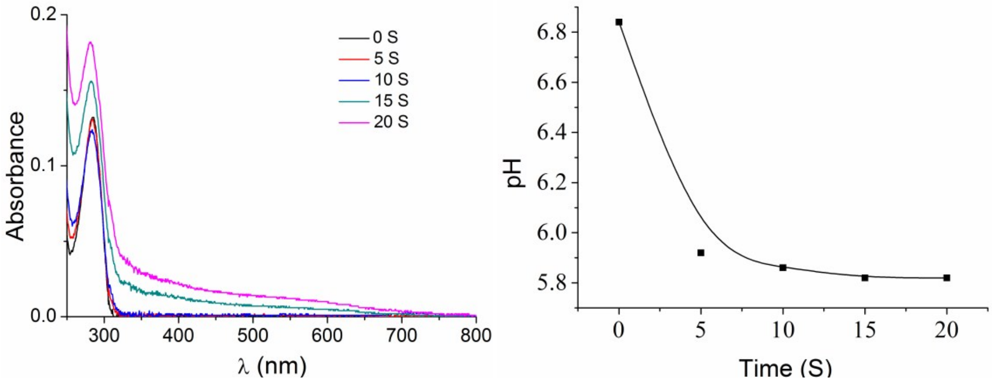

Figure S25. The absorption spectra and pH change of bcm-bpy (10 μM in H_2O) under irradiation (λ_{irr}= 254 nm).

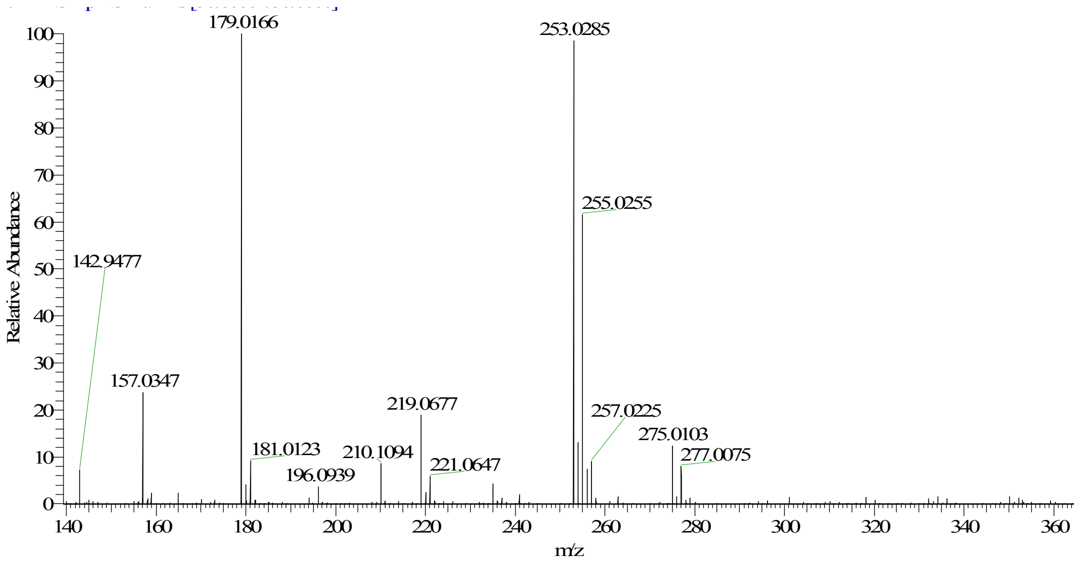

Figure S26. Mass spectrum of bcm-bpy after 254 nm irradiation. The peak of 253.0285 could be ascribed to the bcm-bpy (cal. =253.1272), while other peaks are hard to be analyzed.

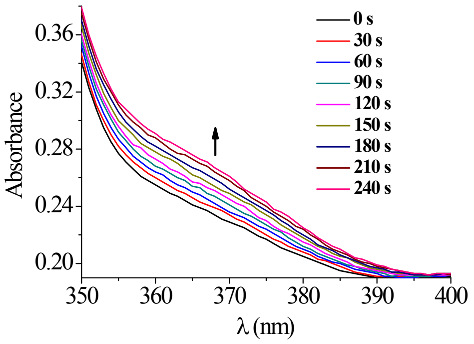

Figure S27. Absorption spectra changes of the solution containing **3** (10 μM), MUP (83.3 μM) and acid phosphatase (0.08 mg/mL) after irradiation (520 nm LED).

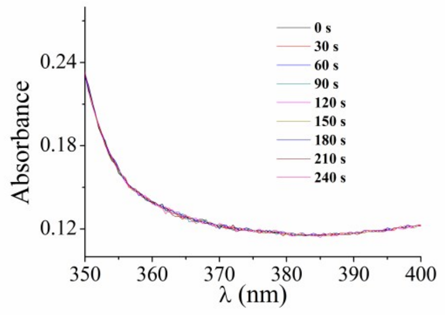

Figure S28. Absorption spectra changes of the solution containing **3** (10 μM), MUP (83.3 μM) after irradiation (520 nm LED).

References

1 N. Tian, W. Sun, X. Guo, Jian, Lu, C. Li, Y. Hou, X. Wang, Q. Zhou, *Chem. Commun.,* 2019, **55**, 2676-2679.

2 M. J. Frisch, G. W. Trucks, H. B. Schlegel, G. E. Scuseria, M. A. Robb, J. R. Cheeseman, G. Scalmani, V. Barone, B. Mennucci, G. A. Petersson, H. Nakatsuji, M. Caricato, X. Li, H. P. Hratchian, A. F. Izmaylov, J. Bloino, G. Zheng, J. L. Sonnenberg, M. Hada, M. Ehara, K. Toyota, R. Fukuda, J. Hasegawa, M. Ishida, T. Nakajima, Y. Honda, O. Kitao, H. Nakai, T. Vreven, J. A. Montgomery Jr., J. E. Peralta, F. Ogliaro, M. Bearpark, J. J. Heyd, E. Brothers, K. N. Kudin, V. N. Staroverov, R. Kobayashi, J. Normand, K. Raghavachari, A. Rendell, J. C. Burant, S. S. Iyengar, J. Tomasi, M. Cossi, N. Rega, J. M. Millam, M. Klene,

J. E. Knox, J. B. Cross, V. Bakken, C. Adamo, J. Jaramillo, R. Gomperts, R. E. Stratmann, O. Yazyev, A. J. Austin, R. Cammi, C. Pomelli, J. W. Ochterski, R. L. Martin, K. Morokuma, V. G. Zakrzewski, G. A. Voth, P. Salvador, J. J. Dannenberg, S. Dapprich, A. D. Daniels, Ö. Farkas, J. B. Foresman, J. V. Ortiz, J. Cioslowski, D. J. Fox, *Gaussian 09, revision A.1, Gaussian, Inc., Wallingford, CT*, 2009.

3 a) A. D. Becke, *J. Chem. Phys.,* 1993, **98**, 5648-5652. b) C. Lee, W. Yang, R. G. Parr, *Phys. Rev. B: Condens. Matter*., 1988, **37**, 785-789.

4 M. Montalti, A. Credi, L. Prodi, M. T. Gandolfi, *Handbook of photochemistry, 3rd ed*., CRC Press: Boca Raton, 2006, Chapter 12.

5 S. Kohse, A. Neubauer, A. Pazidis, S. Lochbrunner, U. Kragl, *J. Am. Chem. Soc*., 2013, **135**, 9407-9411.